

Cosmic Chandlery with Thermonuclear Supernovae

A C Calder^{1,2}, B K Krueger³, A P Jackson¹, D E Willcox¹,
B J Miles⁴ and D M Townsley⁴

¹ Department of Physics and Astronomy, Stony Brook University, Stony Brook, NY
11794-3800, USA

² Institute for Advanced Computational Science, Stony Brook University, Stony Brook, NY
11794-5250, USA

³ XCP-2, Los Alamos National Laboratory, Los Alamos, NM 87545, USA

⁴ Department of Physics and Astronomy, University of Alabama, Tuscaloosa, AL 35487-0324,
USA

E-mail: alan.calder@stonybrook.edu

Abstract. Thermonuclear (Type Ia) supernovae are bright stellar explosions, the light curves of which can be calibrated to allow for use as “standard candles” for measuring cosmological distances. Contemporary research investigates how the brightness of an event may be influenced by properties of the progenitor system that follow from properties of the host galaxy such as composition and age. The goals are to better understand systematic effects and to assess the intrinsic scatter in the brightness, thereby reducing uncertainties in cosmological studies. We present the results from ensembles of simulations in the single-degenerate paradigm addressing the influence of age and metallicity on the brightness of an event and compare our results to observed variations of brightness that correlate with properties of the host galaxy. We also present results from “hybrid” progenitor models that incorporate recent advances in stellar evolution.

1. Introduction

Supernovae are bright stellar explosions that signal the violent deaths of stars. These events synthesize heavy elements, may be a site of r-process nucleosynthesis, and create neutron stars and black holes, which are the building blocks of other interesting astrophysical systems such as x-ray binaries. While these events may be divided into multiple classifications observationally, the impetus for the majority of events is understood to be either the release of gravitational binding energy from the collapsing core of a massive star or the release of nuclear binding energy when a thermonuclear runaway incinerates one or more compact stars. Accordingly, these two mechanisms are referred to as “core collapse” and “thermonuclear,” respectively, and together these produce and disseminate the majority of heavy elements found in the galaxy and thereby drive galactic chemical evolution. Core collapse supernovae create neutron stars and black holes and may be a site of r-process nucleosynthesis, while thermonuclear supernovae completely disrupt the progenitor, leaving only an unbound remnant. Thermonuclear supernovae are particularly useful as distance indicators for cosmological studies, making understanding these events and properties such as their intrinsic scatter important to fields well beyond stellar astrophysics. This manuscript reports on studies of systematic effects on the brightness of thermonuclear supernovae that follow from the evolutionary history of the progenitor star and

host galaxy, with the goal of better constraining uncertainty in the intrinsic scatter of these events.

1.1. Thermonuclear Supernovae

Thermonuclear supernovae are understood to follow from a thermonuclear runaway involving roughly one solar mass of stellar material under degenerate conditions. Discerning the setting(s) of these events, however, is proving to be difficult. Thermonuclear supernovae are unique among supernovae in that they are also very important for cosmological studies because their observational properties (e.g. the light curve) allow calibration of events for use as “standard candles,” i.e. objects of known brightness that may be used as distance indicators. Using thermonuclear supernovae in this capacity resulted in the discovery of the accelerating expansion of the Universe and thus the mysterious dark energy driving the acceleration [1, 2, 3].

Observationally, thermonuclear supernovae are classified as “Type Ia” following the classification scheme of Minkowski [4]. The classification is based on observing strong Si lines and a lack of H in the spectrum of an event. Theoretically, these events are understood to follow from the thermonuclear incineration of $\simeq 1 M_{\odot}$ of a mixture principally composed of C and O under degenerate conditions. The burning converts much of the material to iron-group elements (IGEs) including $\sim 0.6 M_{\odot}$ of radioactive ^{56}Ni , the decay of which powers the light curve [5, 6, 7, 8]. The ability to standardize the light curves is understood to follow from the fact that the source powering the light curve, radioactive ^{56}Ni , is also the principal source of opacity [9]. The result is that the B-band magnitude of the light curves of brighter events decline more slowly from peak than those of dimmer events. This “brighter is broader” result is known as the Phillips relation [10], and it allows the calibration of light curves via a single-parameter “stretch” function [11].

Largely motivated by cosmological studies, many contemporary campaigns are observing Type Ia supernovae. Observations suggest that there may be systematic effects on the peak magnitude of the light curve even after calibration [12], which is a significant source of uncertainty in cosmological studies utilizing these as distance indicators. Spectral diversity raises the possibility of two populations, which may follow from formation channel or from properties of the host galaxy and/or the local environment within the host galaxy. Arguments are made for two populations [13, 14, 15] or for correlation principally with age measured as the delay time from early star formation in a galaxy [16, 11, 17, 18].

One key measure in these studies is the amount of metals, elements heavier than He, that were synthesized by previous generations of stars. The presence of metals influences the evolution of stars and stellar explosions by increasing the number of pathways for nuclear burning [19]. The metallicity of a particular galaxy increases with age, and within a particular galaxy metallicity changes with location, generally increasing toward the densely populated interior. In addition, observations of specific events also can address the issue of progenitors, with some bright observations suggesting more radioactive ^{56}Ni than could be produced by degenerate C and O in a single star [20, 21, 22, 23].

Although many of these events have been observed and these events serve as the premier cosmological distance indicators, a robust theoretical understanding remains elusive. It is widely accepted that compact stars known as white dwarfs (WDs) composed principally of C and O provide the nuclear fuel, but the progenitor systems have not been conclusively identified and questions about the mechanism of the explosion remain. The three most widely accepted proposed progenitor systems are: a single near-Chandrasekhar-mass WD that has gained mass from a companion (the “single degenerate” scenario), the merger of two WDs, and the sub-Chandrasekhar-mass double-detonation scenario in which a detonation in an accreted layer triggers a detonation in the core of the WD [24, and references therein]. For studies of systematic effects, we have adopted the single-degenerate model.

1.2. The Single-Degenerate Explosion Paradigm

The single-degenerate scenario encompasses several explosion mechanisms invoking both deflagrations (subsonic burning fronts) and detonations (supersonic burning fronts). The key to a successful explosion, the production of an unbound remnant with a stratified composition structure similar to observed remnants [25], is the density at which the material of the WD burns. Some of the earliest work addressing the single-degenerate progenitor explored pure detonations and found that the result is the vast majority of the WD material burns to IGEs because of the relatively high density of the WD [26]. In this case, there is no composition stratification in the remnant, and, accordingly, pure detonations have been ruled out as a viable explosion mechanism for some time.

Pure deflagrations have also been explored as the explosion mechanism. In this case, the star reacts to the subsonic burning and expands, which lowers the density of the material prior to it being consumed. The density in the outer regions of the star gets low enough to quench the burning, and the result is an incompletely-burned, bound object that does not release enough energy to explain the majority of observed Type Ia supernovae [27]. Pure deflagrations may explain some unusual events, however [28].

Because the two extremes of pure deflagrations or pure detonations cannot robustly reproduce events with characteristics consistent with the observations, researchers have investigated models evoking a combination of the two. These models may be broadly described as delayed detonation, and a variety of scenarios have been proposed. The classic delayed detonation model was introduced by Khokhlov [29, 30, 31], and variations include pulsational detonations [32, 29, 33, 34, 35], gravitationally confined detonation [36, 37, 38], and deflagration-to-detonation transitions (DDTs) [39, 29, 40, 41, 42, 43]. We adopt a variation of the latter case, a deflagration-to-detonation transition that occurs at the top of a rising plume of hot, burned material when it reaches a threshold density.

The physics by which a DDT may occur are not completely understood, but ideas have been proposed. One idea is that at low densities the flame enters a regime of distributed burning in which it is no longer well-defined but the net burning rate is high enough that it is effectively supersonic [40]. Similarly, others argue that when the flame reaches a certain fractal dimension, it is effectively supersonic [44]. The Zel'dovich mechanism posits that composition and temperature gradients may “prepare” the fuel in just the right way that it will detonate [45, 46, 47]. Our approach is to assume that when the top of a rising, Rayleigh-Taylor unstable plume reaches a particular density, conditions are favorable and the transition occurs [48].

2. Simulation Instrument

The simulations of thermonuclear supernovae we describe here were performed with a modified version of the Flash code, developed at the University of Chicago.¹ Flash is a parallel, adaptive mesh, multi-physics simulation code developed first for nuclear astrophysics applications and subsequently for high-energy-density applications [49, 50, 51, 52, 53]. The modifications to the Flash code for supernova simulations comprise routines to describe thermonuclear burning during both the deflagration and detonation phases, as well as routines to describe the evolution of the dynamic ash.

The significant disparity between radius of a white dwarf ($\sim 10^9$ cm) and the width of laminar nuclear flame at high densities (< 1 cm) requires the use of a model during the deflagration phase because even with many orders of refinement on an adaptive mesh, a macroscopic simulation of the event cannot resolve the actual flame front. Our model propagates an artificially broadened flame with an advection-diffusion-reaction (ADR) scheme [54, 55] via evolution of a reaction

¹ The source code used for these studies is available as a package compatible with the current Flash code from <http://astronomy.ua.edu/townsley/code>.

progress variable ϕ , where $\phi = 0$ indicates unburned fuel and $\phi = 1$ indicates burned ash. The advection-diffusion-reaction equation is

$$\partial_t \phi + \vec{u} \cdot \nabla \phi = \kappa \nabla^2 \phi + \frac{1}{\tau} R(\phi), \quad (1)$$

where \vec{u} is the velocity of the fluid, κ is the diffusion coefficient, τ is the reaction timescale, and $R(\phi)$ is a non-dimensional function. The diffusion and reaction parameters κ , τ , and $R(\phi)$ are tuned to propagate the reaction front at a prescribed speed. We use a modified version of the KPP reaction rate discussed by [55], the “sharpened KPP reaction,” with $R \propto (\phi - \epsilon)(1 - \phi + \epsilon)$, where $\epsilon \simeq 10^{-3}$. This scheme has been shown to be acoustically quiet, stable, and to give a unique flame speed [48]. For the input flame speed, we use tabulated flame speeds from direct numerical simulations of thermonuclear burning [56, 57] and boost these to account for enhancements to the burning from unresolved buoyancy and background turbulence [54, 58, 48, 47].

The ADR scheme describes a model flame, but more is needed to adequately describe the burning in the white dwarf. The burning of C and O under degenerate conditions can be described by three stages. First, C is consumed producing reaction products close to Mg. Then O is consumed along with the ashes of C burning, which produces a mixture of silicon group and light elements that is in a statistical quasi-equilibrium [59, 60, 61]. Finally the silicon-group nuclei are converted to IGEs, reaching full nuclear statistical equilibrium (NSE). Each of these stages is described with separate progress variables and separate relaxation times derived from full nuclear network calculations [62, 63].

In both the quasi-equilibrium and full statistical equilibrium, the creation of light elements via photodisintegration balances the creation of heavy elements via fusion, thus maintaining the equilibrium. Energy can continue to be released as the relative abundances change due to hydrodynamic motion, primarily occurring in rising plumes of hot burned material, which changes the local conditions such as density and temperature and thereby adjusts the equilibrium. Electron capture also influences the evolution in three ways: by shifting the binding energy of the material and thereby changing the temperature due to released energy, by changing the Fermi energy and thus the pressure, and by emitting neutrinos that escape and remove energy. Also, electron captures neutronize the material, which produces more neutron rich iron-group material at the expense of ^{56}Ni . As we will see below, this process has a significant impact on the ^{56}Ni yield and thus the brightness of an event. Our flame capturing scheme incorporates these effects via tabulated results from NSE calculations, the details of which may be found in [64]. With all of this included physics, our scheme is able to describe dynamic evolution of the ash in addition to the stages of C-O burning.

In addition to modeling the burning during the deflagration phase, our burning scheme also describes detonations [65, 66] via progress variables. In this case, we use thermally-activated burning with the actual temperature-dependent rate for C consumption to allow a propagating shock to trigger burning, i.e. to propagate a detonation front. In our scheme, the propagating detonation is able to describe the same stages of C burning as the deflagration case, including the relaxation into NSE [63, and references therein].

3. Systematic Effects on the Brightness of an Event

We investigate systematic effects on the brightness of thermonuclear supernovae in the single-degenerate, DDT paradigm (described above). Figure 1 illustrates the progression of thermonuclear burning during a simulation in the DDT paradigm with a massive C-O progenitor WD. The left panel shows the flame during the early deflagration stage with the obvious development of fluid instabilities. The middle panel shows the flame as the first rising bubble reaches the DDT threshold density (marked by the contour). The third panel shows the propagation of two detonations. In all panels, the color scheme shows the composition.

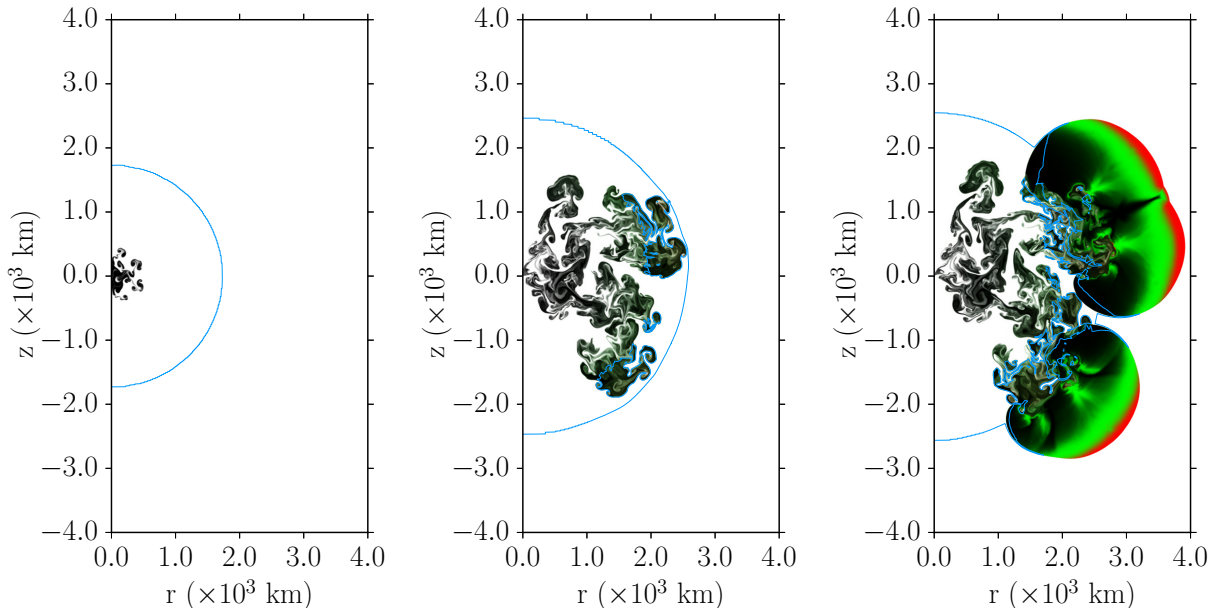


Figure 1. Deflagration to detonation burning progress shown for a C-O WD with $\rho_{\text{DDT}} = 10^{7.2} \text{ g/cm}^3$ (blue contour). Unburned ^{12}C & ^{16}O fuel is shown in white, and ash from ^{12}C -burning is shown in red. Matter in a quasi-nuclear statistical equilibrium state (primarily intermediate-mass silicon-group elements) is represented in green. Finally, matter in nuclear statistical equilibrium (IGEs and α -particles) is shown in black. From left to right, the burning is shown at 0.75 s, 1.74 s, and 1.84 s after the deflagration is initiated.

We note that an important part of our methodology is to perform suites of simulations in order to investigate statistically-significant trends. In [66] we presented a theoretical framework for these investigations utilizing multiple realizations from randomized initial conditions. Our results have shown that the problem of thermonuclear supernovae in the single-degenerate DDT paradigm is deeply nonlinear, particularly during the deflagration phase, which involves competition between the growth of fluid instabilities and evolution of the flame. Accordingly, these models exhibit a significant degree of variability, necessitating a statistical approach [67]. Finally, we note that all of the supernova explosions presented here are from two-dimensional simulations. We found the large number of simulations needed in ensembles necessitated the use of two-dimensional models to be computationally tractable.

3.1. Effect of Composition

The simplest description of burning in a C-O WD is the alpha chain, a series of alpha capture reactions of the form $X(\alpha, \gamma)Y$ going through symmetric nuclei ($n = p$) from ^{12}C and ^{16}O all the way to ^{56}Ni . The presence of metals has been known for some time to boost burning rates in WDs by offering additional burning channels beyond just these basic reactions. In addition, metals are neutron rich, and the neutron excess tends to drive the burning away from symmetric nuclei. The result is that the presence of metals affects the brightness of an event in two ways—faster flame speeds lead to different dynamics during the explosion and neutron excess suppresses ^{56}Ni production.

Metal enrichment of the progenitor WD follows from two sources. First, metals present in the massive star that evolved to become the WD will be present in the progenitor WD. Second, convective burning or “simmering” as the progenitor WD approaches the Chandrasekhar limit synthesizes metals. In simulations, we use ^{22}Ne as a proxy for neutron rich metals in the WD

progenitor originating from both sources.

Based on essentially a counting argument, [68] found that the presence of ^{22}Ne directly modifies the ^{56}Ni abundance during thermonuclear burning of a WD. Our models allow the investigation of the (nonlinear) effects of metallicity on hydrodynamic models. As noted above, metallicity boosts the burning rate by providing an increased number of reaction channels. Accordingly, the flame speeds in explosion models are increased. The increased flame speed changes the dynamics of the deflagration phase and also will change the DDT density, which follows from a competition between the development of fluid instabilities at the flame front and fire polishing. In [66], we explored the role of ^{22}Ne , incorporating its effect on progenitor structure, laminar flame speed, and energy release into simulations. We found that these influence the duration of the deflagration phase, which in turn influences the amount of expansion prior to the detonation that incinerates the star. The amount of expansion determines the overall density structure, and in particular the amount of mass at densities high enough to burn all the way to IGEs. Thus we found metallicity does influence the yield of ^{56}Ni , but we found that these effects were relatively weak. In [69], we included the effect of the changing flame speed on the DDT density. In this case, we found a more drastic effect on the duration of the deflagration phase and, accordingly, on the yield of ^{56}Ni . Figure 2 shows results from these two studies along with observational results for comparison.

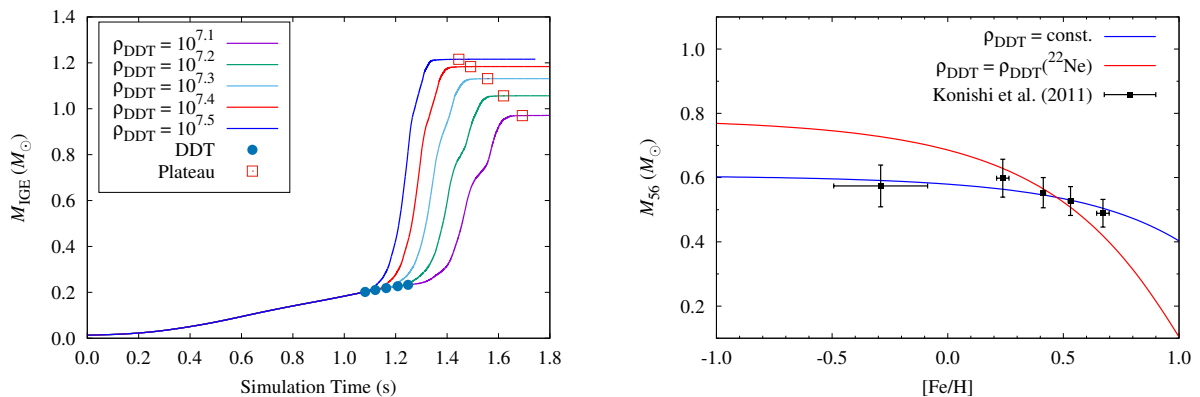


Figure 2. Left panel: Plot of IGE yield vs. time from simulation of the same realization with the DDT density changing to account for increased flame speeds due to increased metallicity. Right panel: Plot of produced mass of ^{56}Ni vs. metallicity comparing simulations to the observational results of [70] (black points). Both panels adapted from [69].

3.2. Effect of Central Density

In [71] and subsequently in [72] we investigated the role of central density on the yield of ^{56}Ni and thus the brightness. Our study constructed models with varying central densities and simulated explosions from these. We found that the overall production of IGEs is statistically independent of progenitor central density, but the mass of stable IGEs is tightly correlated with central density, with a decrease in the production of ^{56}Ni at higher central densities. Thus our results indicate that progenitors with higher central densities produce dimmer events. Our understanding of the source of this trend is the increased neutronization that occurs due to the faster rates of weak reactions at higher densities. By applying the relationship of Lesaffre, et al. [73], which relates the duration of WD cooling prior to the onset of accretion to the central density of the progenitor at ignition, we were able to obtain a relationship between the central density and the cooling time, a significant fraction of the age of the progenitor. With this

relationship, we then had relationships between the cooling time and the masses of IGEs and ^{56}Ni .

Results from the central density study are shown in Figure 3. The left panel shows the mass of ^{56}Ni produced in the explosion from progenitors at 5 central densities for 30 realizations each. The right panel shows relationship between age and stretch, a measure of the brightness when considering the Phillips relation [11]. Also shown are the observational results of Neill, et al. [17] for comparison. An obvious result to note is that the trends agree, but our stretches or yields are consistently higher. While evidence suggests that explosions in the single-degenerate paradigm tend to be bright [43], we attribute the difference as primarily due to our choice of DDT density for the suite of simulations.

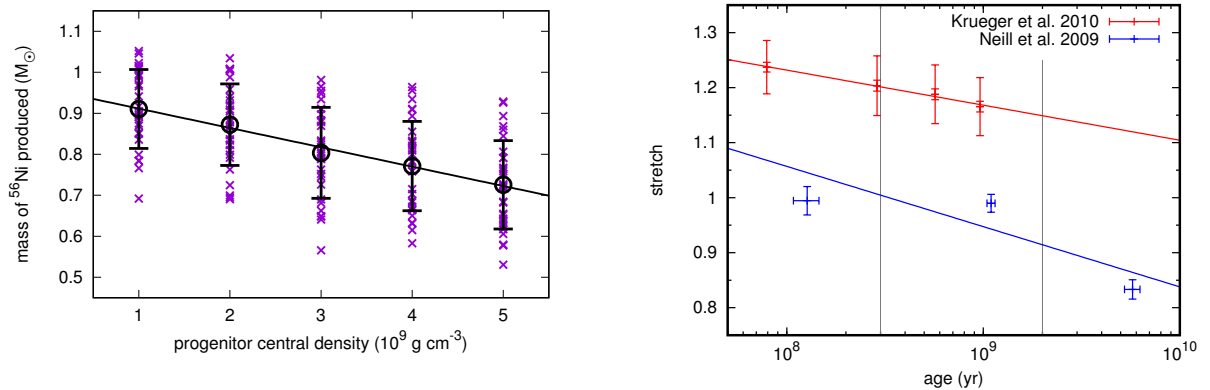


Figure 3. Left panel: Mass of ^{56}Ni as a function of progenitor central density for 30 simulations at each central density. The black lines are the best-fit trend lines with averages and standard deviations marked by the circles and vertical error bars. Right panel: Plots of stretch vs. age with the standard deviation, the standard error of the mean, and a best-fit trend line. In blue are results from Figure 5 of [17] along with a best-fit trend line, and the vertical gray lines mark the cuts between bins. The overall offset to larger stretch in our simulations follows primarily from the choice of DDT density. Adapted from [71].

3.3. Explosions from “Hybrid” Progenitors

Recent work in stellar evolution posits the existence of “hybrid” C-O-Ne white dwarfs consisting of a C core surrounded by a mixture of O and Ne. The structure of these white dwarfs follows from convective boundary mixing quenching a C-flame before it can consume all of the C in the late stages of a super asymptotic giant branch star’s life [74]. C burning produces ^{20}Ne that, because of the convective boundary, remains at a larger radius than the unburned C. The result is a hybrid C-O-Ne WD with more mass than a C-O WD (and thus less mass is needed from accretion to approach the Chandrasekhar limit) [75]. During accretion, C burning commences and drives convection that mixes and removes this layering. The result of this simmering is a progenitor WD with a C-depleted core that is cooler than the surrounding material due to energy loss from neutrino emissions. It differs from a C-O progenitor in its temperature profile and because it has a significant amount of ^{20}Ne . Simulating thermonuclear supernovae from these hybrid progenitors thus required adapting the burning module (described above) to account for the ^{20}Ne [76], and these adaptations were incorporated into the source code to be distributed. We note that studies of these hybrid models continue, and very recent work [77] suggests that mixing during the cooling phase of the WD before the onset of accretion plays an important role and may produce progenitors different in composition and structure from the hybrid models we employed in our study.

We investigated the viability of these hybrid progenitors with a series of explosion simulations in [76]. Figure 4 shows the progression of thermonuclear burning during a simulation similarly to the C-O case illustrated in Figure 1. The panels show the early deflagration phase (left), the moment of ignition of the detonation (center) and the propagation of the detonation (right). An obvious difference between the hybrid progenitor and the C-O case is the cool, C-depleted core, which shows little burning (the “hole” in the center of the star seen in each panel) because the deflagration is born in the high-temperature shell above the core. By the end of the simulation, however, these models eventually consume the core during the detonation phase. A noticeable difference from the C-O models is this delay in burning the inner core.

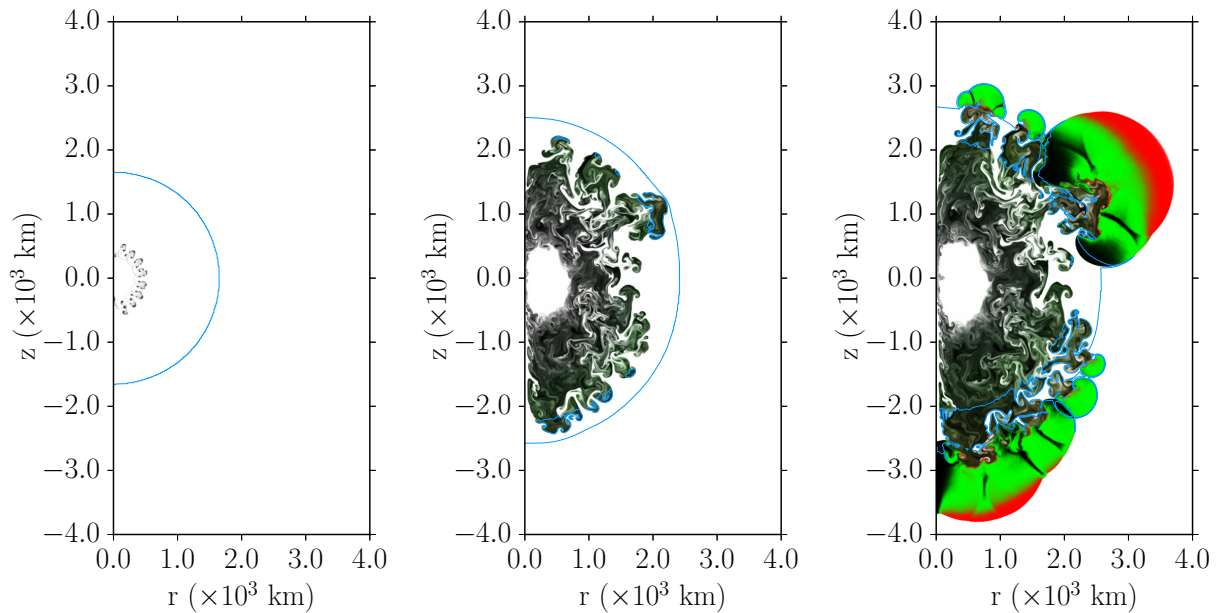


Figure 4. Deflagration to detonation burning progress shown for a C-O-Ne hybrid WD with $\rho_{\text{DDT}} = 10^{7.2} \text{ g/cm}^3$. The color scheme is the same as that of Figure 1. From left to right, the burning is shown at 0.50 s, 1.48 s, and 1.60 s after the deflagration is initiated.

We found that while there can be considerable variability in the outcome, there are statistically significant trends, with hybrid C-O-Ne models having a lower ^{56}Ni yield and ejecta with lower kinetic energy than similar C-O models. Figure 5 illustrates these trends, with the left panel presenting estimated ^{56}Ni yields and the right panel presenting gravitational binding energy. We concluded that these hybrid progenitors are viable for supernova explosions.

3.4. Analysis via Synthetic Spectra and Light Curves

The flame capturing and energetics scheme described above is sufficient to capture the bulk energetics of the explosion and to estimate the yield of ^{56}Ni and IGEs. Making accurate calculations of the abundances synthesized in an explosion, however, requires much higher fidelity calculations of the thermonuclear burning. We address this issue by postprocessing fluid element histories (temperature and density) from Lagrangian tracer particles embedded in the hydrodynamic flow during a supernova simulation. In [63] we presented a new method for this process with particular attention given to reconstructing the fluid element history within the artificially-thickened model flame. We provided details of the method and verification tests demonstrating that for the problem of deflagration and detonation fronts propagating in a uniform medium, we find good agreement between the post-processing method and a direct simulation of the burning.

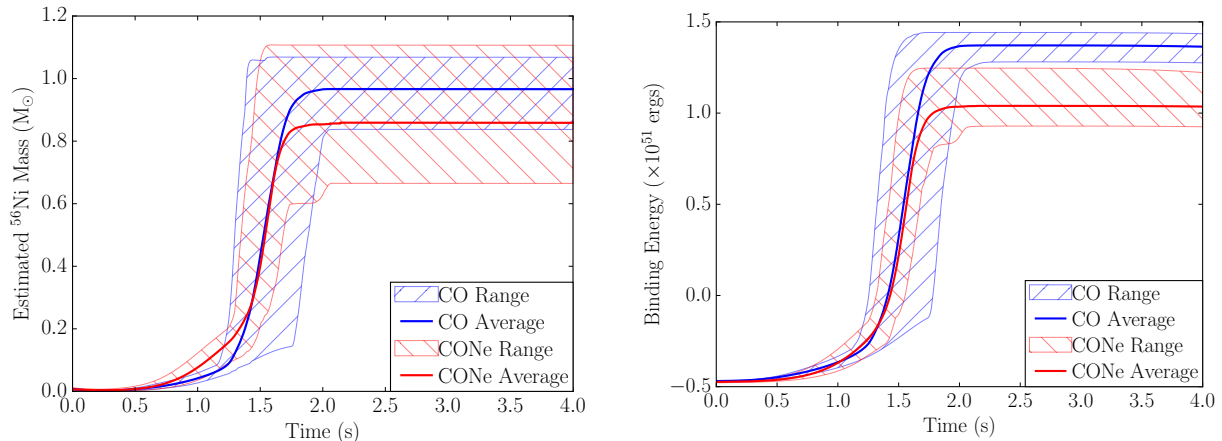


Figure 5. ^{56}Ni yield and gravitational binding energy from suites of simulations of explosions from hybrid C-O-Ne progenitors. The left panel shows the yield of ^{56}Ni from suites of simulations from C-O progenitors (very similar to those of [72]) and from C-O-Ne hybrid progenitors. The right panel shows the binding energy from the two suites. In both panels, the range of results are marked by the hashed regions. Adapted from [76].

With these accurate, detailed abundances, we were able to generate synthetic spectra from our post-processed explosion models to compare with observations in order to explore how signatures of metallicity in the spectral features may be used to constrain the metallicity of the progenitor WD [78]. We performed explosion simulations from progenitors for a range of metallicities, and from the spectra were able to find correlations between the progenitor metallicity and the strength of certain spectral features. Specifically, a Ti feature near 4200 Å and an Fe feature near 5200 Å show a trend of increasing width with increasing metallicity. These results suggest the ability to observationally differentiate between progenitor metallicities.

Figure 6 shows synthetic spectra from post-processed remnants derived from simulations at different metallicities. The top panel shows spectra at 10, 20, 30, and 40 days after the explosion. The middle and bottom panels show spectra from post-processed remnants at 30 days after the explosion that were derived from simulations at low and high metallicities, respectively. The spectra at the two metallicities are “knock out” spectra calculated with and without the contribution to the opacity from an individual transition line [79]. The two knock out spectra are from the same DDT realization simulated at the two metallicities. Changes in the differences between the model spectra and “knock out” spectra serve as a diagnostic for changes following from varying metallicity.

4. Conclusions

We have developed a detailed flame-capturing and energetics scheme to model thermonuclear supernovae and coupled it to post-processing techniques to calculate detailed abundances and synthetic spectra and light curves. With these tools, we have investigated systematic effects on the brightness of thermonuclear supernovae (in the single-degenerate DDT paradigm) that are thought to follow from the evolutionary history of the progenitor star and host galaxy. We investigated the effects of age and composition and our results are in rough agreement with observed trends. We also were able to quantify variations within the suites of simulations and thereby evaluate the variability of these models. While our results are prior to calibration by the Phillips relation, understanding these first-order effects on the brightness is a significant step toward assessing the intrinsic scatter of these events.

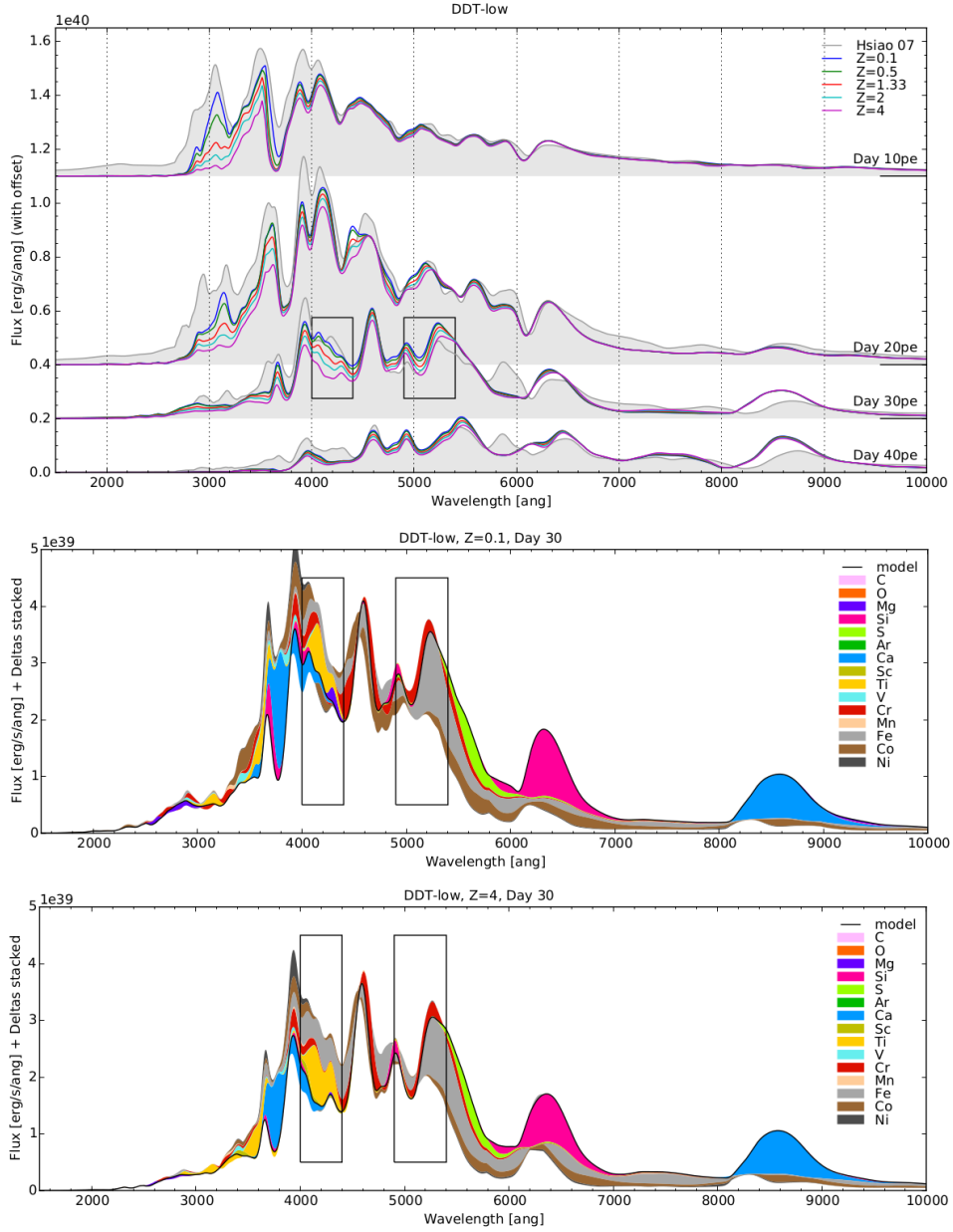


Figure 6. Spectra from a suite of simulations at varying metallicity at 10, 20, 30, and 40 days after the explosion illustrating evolution (top panel). Also shown are “knockout” spectra from one DDT realization simulated with metallicity $Z/Z_{\odot} = 0.1$ (middle panel) and $Z/Z_{\odot} = 4.0$ (bottom panel) at 30 days after the explosion. Contributions from line opacity of individual elements to the full spectrum (black solid lines) are represented by colored patches. These are calculated by removing the line opacities from a single element and recalculating the spectra while keeping the temperatures and population numbers fixed. Emission contributions are represented by colored patches below the full spectra, and absorption contributions are represented by patches above the full spectra. The spectral features highlighted with black boxes indicate two potential spectral indicators for progenitor metallicity. Adapted from [78].

We also investigated explosions from hybrid C-O-Ne progenitors and found that these

progenitors produce explosions similar to explosions from traditional C-O progenitors, but with a slightly lower yield of ^{56}Ni and ejecta with slightly lower kinetic energy. The viability of these models is significant in that the hybrid progenitors require less accreted mass and thereby ameliorate a concern with the single-degenerate paradigm.

In the future, we will use these tools to explore simulations from more realistic progenitors as these become available. We are presently performing a study of the convective Urca process with fully three-dimensional simulations. Introduced by Paczyński [80], the convective Urca process occurs when neutrino losses alter the dynamics of convection, in this case in the simmering progenitor WD [81, 82, 83, 84]. The process occurs in a region of the star known as the “Urca shell.” Above the density of the shell, electron capture is favorable due to the high Fermi energy, while below this density β -decay occurs. Generally an Urca shell is specific to an Urca pair of nuclides, and a pair that is important for thermonuclear supernova progenitors is $^{23}\text{Ne}/^{23}\text{Na}$. The effect of the Urca shell is twofold—energy is lost to neutrinos and the shell forms a barrier to buoyancy because of the different nucleon/electron ratio across the shell. Through these two effects the Urca shell can influence both the energy content of the star and the flow structure in the convection zone. The results of our study will inform progenitor models for future explosion simulations that will address the effects of these results on the brightness of events.

Acknowledgments

The work described in this paper is a distillation of parts of a large effort exploring thermonuclear supernovae. The authors gratefully acknowledge contributions from Frank Timmes, Ed Brown, David Chamulak, Daan van Rossum, Shimon Asida, Ivo Seitenzahl, Fang Peng, Natalia Vladimirova, Don Lamb, and Jim Truran. This work was supported in part by the US Department of Energy under grants DE-FG02-07ER41516 and DE-FG02-87ER40317. This work was supported in part by the US National Science Foundation under grant AST-0507456. This work was supported in part by the US National Aeronautics and Space Administration under grant NNX09AD19G. D.M.T. received support from the Bart J. Bok fellowship at the University of Arizona for part of this work. A.P.J. received support from a National Research Council Research Associateship for part of this work. The authors acknowledge the hospitality of the Kavli Institute for Theoretical Physics, which is supported by the NSF under grant PHY05-51164, during the programs “Accretion and Explosion: the Astrophysics of Degenerate Stars” and “Stellar Death and Supernovae.” The software used in this work was in part developed by the DOE-supported ASC/Alliances Center for Astrophysical Thermonuclear Flashes at the University of Chicago. Results in this paper were obtained using the high-performance computing system at the Institute for Advanced Computational Science at Stony Brook University and via US National Science Foundation TeraGrid and US Department of Energy INCITE awards. The authors also thank Rachel Losacco and Ishmam Yousuf for previewing the manuscript.

References

- [1] Riess A G, Filippenko A V, Challis P, Clocchiatti A, Diercks A, Garnavich P M, Gilliland R L, Hogan C J, Jha S, Kirshner R P, Leibundgut B, Phillips M M, Reiss D, Schmidt B P, Schommer R A, Smith R C, Spyromilio J, Stubbs C, Suntzeff N B and Tonry J 1998 *AJ* **116** 1009 (*Preprint astro-ph/9805201*)
- [2] Perlmutter S, Aldering G, Goldhaber G, Knop R A, Nugent P, Castro P G, Deustua S, Fabbro S, Goobar A, Groom D E, Hook I M, Kim A G, Kim M Y, Lee J C, Nunes N J, Pain R, Pennypacker C R, Quimby R, Lidman C, Ellis R S, Irwin M, McMahon R G, Ruiz-Lapuente P, Walton N, Schaefer B, Boyle B J, Filippenko A V, Matheson T, Fruchter A S, Panagia N, Newberg H J M, Couch W J and The Supernova Cosmology Project 1999 *ApJ* **517** 565 (*Preprint astro-ph/9812133*)
- [3] Leibundgut B 2001 *Annu. Rev. Astron. Astrophys* **39** 67–98
- [4] Minkowski R 1941 *PASP* **53** 224
- [5] Pankey Jr T 1962 *Possible Thermonuclear Activities in Natural Terrestrial Minerals*. Ph.D. thesis HOWARD UNIVERSITY.

- [6] Colgate S A and McKee C 1969 *ApJ* **157** 623
- [7] Colgate S A, Petschek A G and Kriese J T 1980 *ApJ* **237** L81–L85
- [8] Kuchner M J, Kirshner R P, Pinto P A and Leibundgut B 1994 *ApJ* **426** L89
- [9] Pinto P A and Eastman R G 2001 *New Astronomy* **6** 307–319
- [10] Phillips M M 1993 *ApJ* **413** L105
- [11] Howell D A, Sullivan M, Brown E F, Conley A, LeBorgne D, Hsiao E Y, Astier P, Balam D, Balland C, Basa S, Carlberg R G, Fouchez D, Guy J, Hardin D, Hook I M, Pain R, Perrett K, Pritchett C J, Regnault N, Baumont S, LeDu J, Lidman C, Perlmutter S, Suzuki N, Walker E S and Wheeler J C 2009 *ApJ* **691** 661–671 (*Preprint* 0810.0031)
- [12] Kirshner R P 2010 *Foundations of supernova cosmology* p 151
- [13] Mannucci F, Della Valle M and Panagia N 2006 *MNRAS* **370** 773–783 (*Preprint* arXiv:astro-ph/0510315)
- [14] Raskin C, Scannapieco E, Rhoads J and Della Valle M 2009 *ApJ* **707** 74–78 (*Preprint* 0909.4293)
- [15] Wang X, Wang L, Filippenko A V, Zhang T and Zhao X 2013 *Science* **340** 170–173 (*Preprint* 1303.2601)
- [16] Gallagher J S, Garnavich P M, Caldwell N, Kirshner R P, Jha S W, Li W, Ganeshalingam M and Filippenko A V 2008 *ApJ* **685** 752–766 (*Preprint* 0805.4360)
- [17] Neill J D, Sullivan M, Howell D A, Conley A, Seibert M, Martin D C, Barlow T A, Foster K, Friedman P G, Morrissey P, Neff S G, Schiminovich D, Wyder T K, Bianchi L, Donas J, Heckman T M, Lee Y, Madore B F, Milliard B, Rich R M and Szalay A S 2009 *ApJ* **707** 1449–1465 (*Preprint* 0911.0690)
- [18] Brandt T D, Tojeiro R, Aubourg É, Heavens A, Jimenez R and Strauss M A 2010 *AJ* **140** 804–816 (*Preprint* 1002.0848)
- [19] Chamulak D A, Brown E F and Timmes F X 2006 *Proc. Sci.* **submitted**
- [20] Howell D A, Sullivan M, Nugent P E, Ellis R S, Conley A J, Le Borgne D, Carlberg R G, Guy J, Balam D, Basa S, Fouchez D, Hook I M, Hsiao E Y, Neill J D, Pain R, Perrett K M and Pritchett C J 2006 *Nature* **443** 308–311 (*Preprint* arXiv:astro-ph/0609616)
- [21] Scalzo R A, Aldering G, Antilogus P, Aragon C, Bailey S, Baltay C, Bongard S, Buton C, Childress M, Chotard N, Copin Y, Fakhouri H K, Gal-Yam A, Gangler E, Hoyer S, Kasliwal M, Loken S, Nugent P, Pain R, Pécontal E, Pereira R, Perlmutter S, Rabinowitz D, Rau A, Rigaudier G, Runge K, Smadja G, Tao C, Thomas R C, Weaver B and Wu C 2010 *ApJ* **713** 1073–1094 (*Preprint* 1003.2217)
- [22] Yuan F, Quimby R M, Wheeler J C, Vinkó J, Chatzopoulos E, Akerlof C W, Kulkarni S, Miller J M, McKay T A and Aharonian F 2010 *ApJ* **715** 1338–1343 (*Preprint* 1004.3329)
- [23] Tanaka M, Kawabata K S, Yamanaka M, Maeda K, Hattori T, Aoki K, Nomoto K, Iye M, Sasaki T, Mazzali P A and Pian E 2010 *ApJ* **714** 1209–1216 (*Preprint* 0908.2057)
- [24] Calder A C, Krueger B K, Jackson A P and Townsley D M 2013 *Frontiers of Physics* **8** 168–188 (*Preprint* 1303.2207)
- [25] Mazzali P A, Sauer D N, Pastorello A, Benetti S and Hillebrandt W 2008 *MNRAS* **386** 1897–1906 (*Preprint* 0803.1383)
- [26] Arnett W D, Truran J W and Woosley S E 1971 *ApJ* **165** 87
- [27] Röpke F K, Hillebrandt W, Schmidt W, Niemeyer J C, Blinnikov S I and Mazzali P A 2007 *ApJ* **668** 1132–1139 (*Preprint* 0707.1024)
- [28] Kromer M, Ohlmann S T, Pakmor R, Ruiter A J, Hillebrandt W, Marquardt K S, Röpke F K, Seitenzahl I R, Sim S A and Taubenberger S 2015 *MNRAS* **450** 3045–3053 (*Preprint* 1503.04292)
- [29] Khokhlov A M 1991 *A&A* **245** 114–128
- [30] Höflich P, Khokhlov A M and Wheeler J C 1995 *ApJ* **444** 831–847
- [31] Gamezo V N, Khokhlov A M and Oran E S 2005 *ApJ* **623** 337–346 (*Preprint* astro-ph/0409598)
- [32] Ivanova L N, Imshennik V S and Chechetkin V M 1974 *Ap&SS* **31** 497–514
- [33] Arnett D and Livne E 1994 *ApJ* **427** 315–329
- [34] Arnett D and Livne E 1994 *ApJ* **427** 330–341
- [35] Bravo E and García-Senz D 2006 *ApJ* **642** L157–L160 (*Preprint* astro-ph/0604025)
- [36] Plewa T, Calder A C and Lamb D Q 2004 *ApJ* **612** L37–L40
- [37] Jordan IV G C, Fisher R T, Townsley D M, Calder A C, Graziani C, Asida S, Lamb D Q and Truran J W 2008 *ApJ* **681** 1448–1457
- [38] Jordan IV G C, Graziani C, Fisher R T, Townsley D M, Meakin C, Weide K, Reid L B, Norris J, Hudson R and Lamb D Q 2012 *ApJ* **759** 53 (*Preprint* 1202.3997)
- [39] Blinnikov S I and Khokhlov A M 1986 *Soviet Astronomy Letters* **12** 131–+
- [40] Niemeyer J C and Woosley S E 1997 *ApJ* **475** 740 (*Preprint* astro-ph/9607032)
- [41] Niemeyer J C 1999 *ApJ* **523** L57–L60 (*Preprint* arXiv:astro-ph/9906142)
- [42] Bell J B, Day M S, Rendleman C A, Woosley S E and Zingale M 2004 *ApJ* **608** 883–906 (*Preprint* astro-ph/0401247)
- [43] Fisher R and Jumper K 2015 *ApJ* **805** 150 (*Preprint* 1504.00014)

- [44] Woosley S E 1990 *Supernovae* ed A G Petschek pp 182–212
- [45] Zel'Dovich Y B, Librovich V B, Makhviladze G M and Sivashinskii G I 1970 *Journal of Applied Mechanics and Technical Physics* **11** 264–270
- [46] Khokhlov A M, Oran E S and Wheeler J C 1997 *ApJ* **478** 678–+ (*Preprint arXiv:astro-ph/9612226*)
- [47] Jackson A P, Townsley D M and Calder A C 2014 *ApJ* **784** 174 (*Preprint 1402.4527*)
- [48] Townsley D M, Calder A C, Asida S M, Seitzzahl I R, Peng F, Vladimirova N, Lamb D Q and Truran J W 2007 *ApJ* **668** 1118–1131 (*Preprint arXiv:0706.1094*)
- [49] Fryxell B, Olson K, Ricker P, Timmes F X, Zingale M, Lamb D Q, MacNeice P, Rosner R, Truran J W and Tufo H 2000 *ApJS* **131** 273–334
- [50] Calder A C, Curtis B C, Dursi L J, Fryxell B, Henry G, MacNeice P, Olson K, Ricker P, Rosner R, Timmes F X, Tufo H M, Truran J W and Zingale M 2000 *Proceedings of Supercomputing 2000* p <http://sc2000.org>
- [51] Calder A C, Fryxell B, Plewa T, Rosner R, Dursi L J, Weirs V G, Dupont T, Robey H F, Kane J O, Remington B A, Drake R P, Dimonte G, Zingale M, Timmes F X, Olson K, Ricker P, MacNeice P and Tufo H M 2002 *ApJS* **143** 201–229
- [52] Dubey A, Calder A, Fisher R, Graziani C, Jordan G, Lamb D, Reid L, Townsley D and Weide K 2013 *International Journal of High Performance Computing Applications* **27** 360–373 ISSN 1094-3420
- [53] Dubey A, Antypas K, Calder A, Daley C, Fryxell B, Gallagher J, Lamb D, Lee D, Olson K, Reid L, Rich P, Ricker P, Riley K, Rosner R, Siegel A, Taylor N, Weide K, Timmes F, Vladimirova N and Zuhone J 2014 *International Journal of High Performance Computing Applications* **28** 225–237 ISSN 1094-3420
- [54] Khokhlov A M 1995 *ApJ* **449** 695
- [55] Vladimirova N, Weirs G and Ryzhik L 2006 *Combust. Theory Modelling* **10** 727–747
- [56] Timmes F X and Woosley S E 1992 *ApJ* **396** 649
- [57] Chamulak D A, Brown E F and Timmes F X 2007 *ApJ* **655** L93 (*Preprint astro-ph/0612507*)
- [58] Gamezo V N, Khokhlov A M, Oran E S, Chtchelkanova A Y and Rosenberg R O 2003 *Science* **299** 77
- [59] Imshennik V S, Filippov S S and Khokhlov A M 1981 *Soviet Astronomy Letters* **7** 121
- [60] Khokhlov A M 1981 *Soviet Astronomy Letters* **7** 410–413
- [61] Khokhlov A M 1983 *Soviet Astronomy Letters* **9** 160
- [62] Calder A C, Townsley D M, Seitzzahl I R, Peng F, Messer O E B, Vladimirova N, Brown E F, Truran J W and Lamb D Q 2007 *ApJ* **656** 313–332 (*Preprint arXiv:astro-ph/0611009*)
- [63] Townsley D M, Miles B J, Timmes F X, Calder A C and Brown E F 2016 *ApJS* **225** 3 (*Preprint 1605.04878*)
- [64] Seitzzahl I R, Townsley D M, Peng F and Truran J W 2009 *Atomic Data and Nuclear Data Tables* **95** 96–114
- [65] Meakin C A, Seitzzahl I, Townsley D, Jordan G C, Truran J and Lamb D 2009 *ApJ* **693** 1188–1208 (*Preprint 0806.4972*)
- [66] Townsley D M, Jackson A P, Calder A C, Chamulak D A, Brown E F and Timmes F X 2009 *ApJ* **701** 1582–1604 (*Preprint 0906.4384*)
- [67] Calder A C, Krueger B K, Jackson A P, Townsley D M, Timmes F X, Brown E F and Chamulak D A 2011 *Proceedings of SciDAC 2010* (Oak Ridge) URL http://computing.ornl.gov/workshops/scidac2010/2010_SciDAC_Proceedings.pdf
- [68] Timmes F X, Brown E F and Truran J W 2003 *ApJ* **590** L83 (*Preprint astro-ph/0305114*)
- [69] Jackson A P, Calder A C, Townsley D M, Chamulak D A, Brown E F and Timmes F X 2010 *ApJ* **720** 99–113 (*Preprint 1007.1138*)
- [70] Konishi K, Cinabro D, Garnavich P M, Ihara Y, Kessler R, Marriner J, Schneider D P, Smith M, Spinka H, Wheeler J C and Yasuda N 2011 *ArXiv e-prints* (*Preprint 1101.4269*)
- [71] Krueger B K, Jackson A P, Townsley D M, Calder A C, Brown E F and Timmes F X 2010 *ApJ* **719** L5–L9 (*Preprint 1007.0910*)
- [72] Krueger B K, Jackson A P, Calder A C, Townsley D M, Brown E F and Timmes F X 2012 *ApJ* **757** 175 (*Preprint 1208.1986*)
- [73] Lesaffre P, Han Z, Tout C A, Podsiadlowski P and Martin R G 2006 *MNRAS* **368** 187–195 (*Preprint arXiv:astro-ph/0601443*)
- [74] Denissenkov P A, Herwig F, Truran J W and Paxton B 2013 *ApJ* **772** 37 (*Preprint 1305.2649*)
- [75] Denissenkov P A, Truran J W, Herwig F, Jones S, Paxton B, Nomoto K, Suzuki T and Toki H 2015 *MNRAS* **447** 2696–2705 (*Preprint 1407.0248*)
- [76] Willcox D E, Townsley D M, Calder A C, Denissenkov P A and Herwig F 2016 *ApJ* **832** 13 (*Preprint 1602.06356*)
- [77] Brooks J, Schwab J, Bildsten L, Quataert E and Paxton B 2016 *ArXiv e-prints* (*Preprint 1611.03061*)
- [78] Miles B J, van Rossum D R, Townsley D M, Timmes F X, Jackson A P, Calder A C and Brown E F 2016 *ApJ* **824** 59 (*Preprint 1508.05961*)
- [79] van Rossum D R 2012 *ArXiv e-prints* (*Preprint 1208.3781*)

- [80] Paczyński B 1972 *Astrophys. Lett.* **11** 53–+
- [81] Iben Jr I 1978 *ApJ* **219** 213–225
- [82] Iben Jr I 1978 *ApJ* **226** 996–1033
- [83] Iben Jr I 1982 *ApJ* **253** 248–259
- [84] Stein J and Wheeler J C 2006 *ApJ* **643** 1190–1197 (*Preprint astro-ph/0512580*)